Title

Rational frames of minimal twist along space curves under specified boundary conditions

Journal

Advances in Computational Mathematics, 44(5)

ISSN

1019-7168

Authors

Farouki, Rida T

Moon, Hwan Pyo

Publication Date

2018-10-01

DOI

10.1007/s10444-018-9599-3

Peer reviewed

Rational frames of minimal twist along space curves under specified boundary conditions

Rida T. Farouki
Department of Mechanical and Aerospace Engineering,
University of California, Davis, CA 95616, USA.
Hwan Pyo Moon
Department of Mathematics,
Dongguk University–Seoul, Seoul 04620, Republic of Korea.

Abstract

An adapted orthonormal frame $(\mathbf{f}_1(\xi), \mathbf{f}_2(\xi), \mathbf{f}_3(\xi))$ on a space curve $\mathbf{r}(\xi)$, $\xi \in [\,0,1\,]$ comprises the curve tangent $\mathbf{f}_1(\xi) = \mathbf{r}'(\xi)/|\mathbf{r}'(\xi)|$ and two unit vectors $\mathbf{f}_2(\xi), \mathbf{f}_3(\xi)$ that span the normal plane. The variation of this frame is specified by its angular velocity $\boldsymbol{\Omega} = \Omega_1\mathbf{f}_1 + \Omega_2\mathbf{f}_2 + \Omega_3\mathbf{f}_3$, and the *twist* of the framed curve is the integral of the component Ω_1 with respect to arc length. A *minimal twist frame* (MTF) has the least possible twist value, subject to prescribed initial and final orientations $\mathbf{f}_2(0), \mathbf{f}_3(0)$ and $\mathbf{f}_2(1), \mathbf{f}_3(1)$ of the normal–plane vectors. Employing the *Euler–Rodrigues frame* (ERF) — a rational adapted frame defined on spatial Pythagorean–hodograph curves — as an intermediary, an exact expression for an MTF with $\Omega_1 =$ constant is derived. However, since this involves rather complicated transcendental terms, a construction of rational MTFs is proposed by the imposition of a rational rotation on the ERF normal–plane vectors. For spatial PH quintics, it is shown that rational MTFs compatible with the boundary conditions can be constructed, with only modest deviations of Ω_1 about the mean value, by a rational quartic normal–plane rotation of the ERF. If necessary, subdivision methods can be invoked to ensure that the rational MTF is free of inflections, or to more accurately approximate a constant Ω_1. The procedure is summarized by an algorithm outline, and illustrated by a representative selection of computed examples.

Keywords: space curves; adapted orthonormal frames; angular velocity; twist; Pythagorean–hodograph curves; Euler–Rodrigues frames; minimal twist frames.

e–mail addresses: farouki@ucdavis.edu, hpmoon@dongguk.edu

1 Introduction

To uniquely describe the spatial motion of a rigid body, one must specify the variation of its *position* and *orientation* with time. Typically, the path of a distinguished point (e.g., the center of mass) is employed to specify the variation of position as a parametric curve $\mathbf{r}(t)$. To describe the variation of orientation, an orthonormal frame $(\mathbf{f}_1(t), \mathbf{f}_2(t), \mathbf{f}_3(t))$ embedded within the body may be used. If the parameter t represents *time*, the first and second derivatives of $\mathbf{r}(t)$ determine the velocity and acceleration of the body, and the first and second derivatives of the frame $(\mathbf{f}_1(t), \mathbf{f}_2(t), \mathbf{f}_3(t))$ determine its angular velocity and acceleration. For a more general parameterization, the chain rule must be invoked to convert parametric derivatives into physical velocities and accelerations (i.e., derivatives with respect to time).

In many contexts, an *adapted* frame — in which $\mathbf{f}_1(t) = \mathbf{r}'(t)/|\mathbf{r}'(t)|$ is the curve tangent, while $\mathbf{f}_2(t)$, $\mathbf{f}_3(t)$ span the curve normal plane at each point — is desirable. A familiar example is the *Frenet frame* $(\mathbf{t}, \mathbf{n}, \mathbf{b})$ comprising the tangent $\mathbf{t}$, defining the instantaneous direction of motion along the curve; the principal normal $\mathbf{n}$ pointing toward the center of curvature; and the binormal $\mathbf{b} = \mathbf{t} \times \mathbf{n}$ [25]. The angular velocity of the Frenet frame is specified by the *Darboux vector* $\kappa\,\mathbf{b} + \tau\,\mathbf{t}$, where κ and τ are the curvature and torsion [25]. The angular velocity component $\tau\,\mathbf{t}$ specifies the instantaneous rotation rate of the normal plane vectors $\mathbf{n}, \mathbf{b}$ about the tangent $\mathbf{t}$ along the curve.

If $\mathbf{n}, \mathbf{b}$ are replaced by normal–plane vectors $\mathbf{u}, \mathbf{v}$ with no instantaneous rotation about $\mathbf{t}$, we obtain a *rotation–minimizing* adapted frame $(\mathbf{t}, \mathbf{u}, \mathbf{v})$ — also called a *Bishop frame* [1]. Such frames are useful in computer animation, spatial motion planning, construction of swept surfaces, robotics, and related applications. Many approximation schemes for rotation–minimizing adapted frames have been proposed [14, 19, 20, 21, 23, 24, 26, 27, 30, 31, 32] and in recent years greater emphasis has been placed on the identification of space curves that admit *exact* rational rotation–minimizing frames [9, 11, 17, 18] — such curves are necessarily spatial Pythagorean–hodograph (PH) curves [8], since only the PH curves possess rational unit tangents.

The construction of a rotation–minimizing adapted frame on a given curve $\mathbf{r}(t)$ is essentially an *initial value problem* — i.e., specifying the orientation of the normal–plane vector $\mathbf{u}, \mathbf{v}$ at any curve point completely determines their orientation at every other point. Consequently, it is not possible to construct a rotation–minimizing spatial motion of a rigid body along a specified path with prescribed initial *and* final orientations. Therefore, in previous studies

[13, 15] of rational rotation–minimizing rigid body motions with specified initial/final positions and orientations, the path was not defined *a priori*, but was rather determined as an outcome of the construction procedure.

It is often desirable to prescribe both the path geometry and initial/final orientation states for a spatial rigid–body motion. A novel adapted frame is clearly required for this problem. Ideally, this frame would exhibit a *constant angular velocity component* in the curve tangent direction, consistent with the prescribed boundary conditions, but this property is not compatible with a rational dependence of the frame vectors on the curve parameter — even in the case of a curve with a rational RMF $(\mathbf{t}, \mathbf{u}, \mathbf{v})$ the orientation of the MTF normal–plane vectors relative to $\mathbf{u}$ and $\mathbf{v}$ would be specified by trigonometric functions of the arc length. The focus of this study is therefore on rational MTFs that satisfy the boundary conditions, and suppress variations in the rotation rate of the normal–plane vectors about the tangent.

A typical application for this novel type of adapted frame concerns the case of rigid–body motion along a smooth closed curve $\mathbf{r}(t)$, $t \in [\,0, 1\,]$ with $\mathbf{r}(1) = \mathbf{r}(0)$ and also matched first and second derivatives at this point. When a rotation–minimizing frame with a given initial orientation is used to orient the body along such a path, the final instance $(\mathbf{t}(1), \mathbf{u}(1), \mathbf{v}(1))$ does not, in general, coincide with the initial instance $(\mathbf{t}(0), \mathbf{u}(0), \mathbf{v}(0))$ upon reaching the closure point $\mathbf{r}(1) = \mathbf{r}(0)$. With the new type of adapted frame, however, an exact coincidence of the initial and final frames can be achieved.

The plan for the remainder of this paper is as follows. Section 2 reviews some basic properties of spatial PH curves, the Euler–Rodrigues frame (ERF) defined along them, and the twist and inflectional properties of the ERF. The concept of a *minimal twist frame* (MTF), with prescribed initial and final states, is then introduced in Section 3, and a closed–form solution for an MTF with constant angular velocity in the tangent direction is derived. Since this incurs a rather complicated functional form, Section 4 considers the problem of constructing rational MTFs for which the requirement of constant angular velocity is relaxed to minimizing its variation about the mean value. The use of subdivision methods to ensure that rational MTFs are free of inflections, or to further suppress variations of their angular velocity components in the tangent direction, is also discussed. Section 5 provides an algorithm outline for the construction of rational MTFs, and illustrates its implementation by a selection of computed examples. Finally, in Section 6 we summarize the key results of this study, and identify some possible generalizations and open problems that are worthy of further investigation.

2 Spatial Pythagorean–hodograph curves

A spatial Pythagorean–hodograph curve $\mathbf{r}(\xi)$, $\xi \in [\,0,1\,]$ is generated [8] from a quaternion polynomial

$$\mathcal{A}(\xi) \;=\; u(\xi) + v(\xi)\,\mathbf{i} + p(\xi)\,\mathbf{j} + q(\xi)\,\mathbf{k} \tag{1}$$

and its conjugate $\mathcal{A}^*(\xi) = u(\xi) - v(\xi)\,\mathbf{i} - p(\xi)\,\mathbf{j} - q(\xi)\,\mathbf{k}$ by integrating the product

$$\begin{aligned}\mathbf{r}'(\xi) \;&=\; \mathcal{A}(\xi)\,\mathbf{i}\,\mathcal{A}^*(\xi) \;=\; [\,u^2(\xi) + v^2(\xi) - p^2(\xi) - q^2(\xi)\,]\,\mathbf{i} \\ &\quad + 2\,[\,u(\xi)q(\xi) + v(\xi)p(\xi)\,]\,\mathbf{j} \;+\; 2\,[\,v(\xi)q(\xi) - u(\xi)p(\xi)\,]\,\mathbf{k}\,. \end{aligned} \tag{2}$$

The resulting PH curve $\mathbf{r}(\xi)$ has the polynomial parametric speed

$$\sigma(\xi) \;=\; |\mathbf{r}'(\xi)| \;=\; |\mathcal{A}(\xi)|^2 \;=\; u^2(\xi) + v^2(\xi) + p^2(\xi) + q^2(\xi)\,, \tag{3}$$

which specifies the derivative $\mathrm{d}s/\mathrm{d}\xi$ of arc length s with respect to the curve parameter ξ. Hence, the cumulative arc length function

$$s(\xi) \;=\; \int_0^{\xi} \sigma(t)\;\mathrm{d}t$$

is also a polynomial, and the total arc length

$$S \;=\; s(1) \;=\; \int_0^{1} \sigma(t)\;\mathrm{d}t$$

can be exactly computed. We focus here on the lowest–order PH curves that are suitable for free–form design — the spatial PH quintics [12] — which are generated by quadratic quaternion polynomials

$$\mathcal{A}(\xi) \;=\; \mathcal{A}_0(1-\xi)^2 + \mathcal{A}_1 2(1-\xi)\xi + \mathcal{A}_2\xi^2 \tag{4}$$

with coefficients $\mathcal{A}_r = u_r + v_r\,\mathbf{i} + p_r\,\mathbf{j} + q_r\,\mathbf{k}$ for $r = 0, 1, 2$. The parametric speed (3) has the Bernstein coefficients

$$\begin{aligned} \sigma_0 \;&=\; |\mathcal{A}_0|^2\,, \quad \sigma_1 \;=\; \tfrac{1}{2}(\mathcal{A}_0\mathcal{A}_1^* + \mathcal{A}_1\mathcal{A}_0^*)\,, \\ \sigma_2 \;&=\; \tfrac{1}{6}(\mathcal{A}_0\mathcal{A}_2^* + 4\,|\mathcal{A}_1|^2 + \mathcal{A}_2\mathcal{A}_0^*)\,, \\ \sigma_3 \;&=\; \tfrac{1}{2}(\mathcal{A}_1\mathcal{A}_2^* + \mathcal{A}_2\mathcal{A}_1^*)\,, \quad \sigma_4 \;=\; |\mathcal{A}_2|^2\,, \end{aligned}$$

and the Bernstein coefficients of the arc length polynomial $s(\xi)$ are

$$s_0 \;=\; 0 \quad \text{and} \quad s_r \;=\; s_{r-1} + \tfrac{1}{5}\sigma_{r-1}\,, \;\; r = 1, \ldots, 5\,.$$

2.1 Euler–Rodrigues frame on PH curves

The *Euler–Rodrigues frame* (ERF) is an adapted rational orthonormal frame, defined on spatial PH curves [5] through the expression

$$(\mathbf{e}_1(\xi), \mathbf{e}_2(\xi), \mathbf{e}_3(\xi)) \;=\; \frac{(\mathcal{A}(\xi)\,\mathbf{i}\,\mathcal{A}^*(\xi), \mathcal{A}(\xi)\,\mathbf{j}\,\mathcal{A}^*(\xi), \mathcal{A}(\xi)\,\mathbf{k}\,\mathcal{A}^*(\xi))}{|\mathcal{A}(\xi)|^2}\,. \qquad (5)$$

The frame vector $\mathbf{e}_1(\xi)$ is the curve tangent, while $\mathbf{e}_2(\xi)$ and $\mathbf{e}_3(\xi)$ span the normal plane. Compared with the Frenet–Serret frame [25], the ERF has the advantage of being rational in the curve parameter ξ, and non–singular at inflection points (where the curvature vanishes). In terms of the components of the quaternion polynomial (1), the frame vectors (5) are

$$\begin{aligned}
\mathbf{e}_1 \;&=\; \frac{(u^2+v^2-p^2-q^2)\,\mathbf{i} \;+\; 2(uq+vp)\,\mathbf{j} \;+\; 2(vq-up)\,\mathbf{k}}{u^2+v^2+p^2+q^2}\,,\\
\mathbf{e}_2 \;&=\; \frac{2(vp-uq)\,\mathbf{i} \;+\; (u^2-v^2+p^2-q^2)\,\mathbf{j} \;+\; 2(uv+pq)\,\mathbf{k}}{u^2+v^2+p^2+q^2}\,,\\
\mathbf{e}_3 \;&=\; \frac{2(up+vq)\,\mathbf{i} \;+\; 2(pq-uv)\,\mathbf{j} \;+\; (u^2-v^2-p^2+q^2)\,\mathbf{k}}{u^2+v^2+p^2+q^2}\,. \qquad (6)
\end{aligned}$$

For spatial PH quintics, the ERF vectors have a rational quartic dependence on the curve parameter ξ.

The variation of the ERF along $\mathbf{r}(\xi)$ is specified by its angular velocity $\boldsymbol{\omega}$ through the relations

$$\frac{\mathrm{d}\mathbf{e}_1}{\mathrm{d}s} \;=\; \boldsymbol{\omega} \times \mathbf{e}_1\,, \qquad \frac{\mathrm{d}\mathbf{e}_2}{\mathrm{d}s} \;=\; \boldsymbol{\omega} \times \mathbf{e}_2\,, \qquad \frac{\mathrm{d}\mathbf{e}_3}{\mathrm{d}s} \;=\; \boldsymbol{\omega} \times \mathbf{e}_3\,,$$

and when $\boldsymbol{\omega}$ is expressed in terms of the ERF frame vectors as

$$\boldsymbol{\omega} \;=\; \omega_1\mathbf{e}_1 + \omega_2\mathbf{e}_2 + \omega_3\mathbf{e}_3\,, \qquad (7)$$

its components are specified [10] by

$$\begin{aligned}
\omega_1 \;&=\; \mathbf{e}_3 \cdot \frac{\mathrm{d}\mathbf{e}_2}{\mathrm{d}s} \;=\; -\,\mathbf{e}_2 \cdot \frac{\mathrm{d}\mathbf{e}_3}{\mathrm{d}s} \;=\; 2\,\frac{uv' - u'v - pq' + p'q}{\sigma^2}\,,\\
\omega_2 \;&=\; \mathbf{e}_1 \cdot \frac{\mathrm{d}\mathbf{e}_3}{\mathrm{d}s} \;=\; -\,\mathbf{e}_3 \cdot \frac{\mathrm{d}\mathbf{e}_1}{\mathrm{d}s} \;=\; 2\,\frac{up' - u'p + vq' - v'q}{\sigma^2}\,,\\
\omega_3 \;&=\; \mathbf{e}_2 \cdot \frac{\mathrm{d}\mathbf{e}_1}{\mathrm{d}s} \;=\; -\,\mathbf{e}_1 \cdot \frac{\mathrm{d}\mathbf{e}_2}{\mathrm{d}s} \;=\; 2\,\frac{uq' - u'q - vp' + v'p}{\sigma^2}\,. \qquad (8)
\end{aligned}$$

It is convenient to introduce the polynomial

$$h(\xi) \;=\; u(\xi)v'(\xi) - u'(\xi)v(\xi) - p(\xi)q'(\xi) + p'(\xi)q(\xi)\,, \tag{9}$$

so that the ERF angular velocity component in the tangent direction can be written as

$$\omega_1(\xi) \;=\; 2\,\frac{h(\xi)}{\sigma^2(\xi)}\,. \tag{10}$$

Although the normal–plane vectors $\mathbf{e}_2, \mathbf{e}_3$ depend upon the chosen coordinate frame $(\mathbf{i}, \mathbf{j}, \mathbf{k})$, the angular velocity component ω_1 (which defines the rotation rate of $\mathbf{e}_2$ and $\mathbf{e}_3$ about the curve tangent $\mathbf{e}_1$) is *independent* of the adopted coordinate system. A change of coordinates amounts to replacing $\mathcal{A}(\xi)$ by

$$\tilde{\mathcal{A}}(\xi) \;=\; \mathcal{A}(\xi)\,\mathcal{U} \;=\; \tilde{u}(\xi) + \tilde{v}(\xi)\,\mathbf{i} + \tilde{p}(\xi)\,\mathbf{j} + \tilde{q}(\xi)\,\mathbf{k}\,, \tag{11}$$

for some unit quaternion $\mathcal{U}$, and one can verify that the polynomials $\tilde{\sigma}(\xi)$ and $\tilde{h}(\xi)$ generated by substituting $\tilde{u}(\xi), \tilde{v}(\xi), \tilde{p}(\xi), \tilde{q}(\xi)$ for $u(\xi), v(\xi), p(\xi), q(\xi)$ in (3) and (9) are identical to $\sigma(\xi)$ and $h(\xi)$.

2.2 Properties of the Euler–Rodrigues frame

The *twist* T_{ERF} of the ERF represents the total rotation[1] of the normal–plane vectors $\mathbf{e}_2, \mathbf{e}_3$ about the tangent $\mathbf{e}_1$ along $\mathbf{r}(\xi)$, namely

$$T_{\mathrm{ERF}} \;=\; \int_0^S \omega_1\,\mathrm{d}s \;=\; \int_0^1 \omega_1(\xi)\,\sigma(\xi)\,\mathrm{d}\xi \;=\; 2\int_0^1 \frac{h(\xi)}{\sigma(\xi)}\,\mathrm{d}\xi\,. \tag{12}$$

For a PH quintic, the integrand has a numerator of degree 2 and denominator of degree 4, and the integral admits a closed–form reduction through a partial fraction decomposition. Let $\mathbf{z}_1, \overline{\mathbf{z}}_1$ and $\mathbf{z}_2, \overline{\mathbf{z}}_2$ denote the two pairs of complex conjugate roots of the real polynomial $\sigma(\xi) = u^2(\xi) + v^2(\xi) + p^2(\xi) + q^2(\xi)$, so that

$$\sigma(\xi) \;=\; c\,(\xi - \mathbf{z}_1)(\xi - \overline{\mathbf{z}}_1)(\xi - \mathbf{z}_2)(\xi - \overline{\mathbf{z}}_2)$$

for some real constant $c \neq 0$. A closed–form solution for the roots of $\sigma(\xi)$ is possible by means of Ferrari's method [29]. Dividing $h(\xi)$ and $\sigma(\xi)$ by c, the partial–fraction decomposition of the integrand in (12) has the form

$$\frac{h(\xi)}{\sigma(\xi)} \;=\; \frac{\mathbf{c}_1}{\xi - \mathbf{z}_1} + \frac{\overline{\mathbf{c}}_1}{\xi - \overline{\mathbf{z}}_1} + \frac{\mathbf{c}_2}{\xi - \mathbf{z}_2} + \frac{\overline{\mathbf{c}}_2}{\xi - \overline{\mathbf{z}}_2}\,, \tag{13}$$

[1]The term "twist" is established usage in this context, that is of interest in (for example) the geometry of DNA and other complex molecules — see [2, 4, 6, 22].

where the complex values

$$\mathbf{c}_1 \;=\; \frac{h(\mathbf{z}_1)}{(\mathbf{z}_1-\overline{\mathbf{z}}_1)(\mathbf{z}_1-\mathbf{z}_2)(\mathbf{z}_1-\overline{\mathbf{z}}_2)}\,, \quad \mathbf{c}_2 \;=\; \frac{h(\mathbf{z}_2)}{(\mathbf{z}_2-\mathbf{z}_1)(\mathbf{z}_2-\overline{\mathbf{z}}_1)(\mathbf{z}_2-\overline{\mathbf{z}}_2)} \tag{14}$$

are called the *residues* of the rational function $h(\xi)/\sigma(\xi)$ at its poles $\mathbf{z}_1, \mathbf{z}_2$ and $\overline{\mathbf{c}}_1, \overline{\mathbf{c}}_2$ are their conjugates. Then from (13) we have the indefinite integral

$$\int \frac{h(\xi)}{\sigma(\xi)}\,\mathrm{d}\xi \;=\; \mathbf{c}_1 \ln(\xi-\mathbf{z}_1) + \overline{\mathbf{c}}_1 \ln(\xi-\overline{\mathbf{z}}_1) + \mathbf{c}_2 \ln(\xi-\mathbf{z}_2) + \overline{\mathbf{c}}_2 \ln(\xi-\overline{\mathbf{z}}_2)\,,$$

and conjugate terms may be combined to obtain the explicitly real form

$$\begin{aligned}\int \frac{h(\xi)}{\sigma(\xi)}\,\mathrm{d}\xi \;&=\; 2\,\mathrm{Re}(\mathbf{c}_1)\ln|\xi-\mathbf{z}_1| - 2\,\mathrm{Im}(\mathbf{c}_1)\arg(\xi-\mathbf{z}_1) \\ &+\; 2\,\mathrm{Re}(\mathbf{c}_2)\ln|\xi-\mathbf{z}_2| - 2\,\mathrm{Im}(\mathbf{c}_2)\arg(\xi-\mathbf{z}_2)\,. \end{aligned} \tag{15}$$

In utilizing the ERF as a basis for constructing rational MTFs, it is useful to keep in mind some characteristic features that govern the ERF variation. The expression (12) for the twist of the ERF on a spatial PH curve will incur cancellation of clockwise and anti–clockwise rotation of $\mathbf{e}_2, \mathbf{e}_3$ about $\mathbf{e}_1$ if the ERF angular velocity component ω_1 exhibits a sign change for $\xi \in (0,1)$. A point where ω_1 changes sign — i.e., where the polynomial (9) has a real root of odd multiplicity — is called an *inflection* of the ERF. For a PH quintic, this polynomial is quadratic, with the Bernstein coefficients

$$\begin{aligned} h_0 \;&=\; 2(u_0v_1 - u_1v_0 - p_0q_1 + p_1q_0)\,, \\ h_1 \;&=\; u_0v_2 - u_2v_0 - p_0q_2 + p_2q_0\,, \\ h_2 \;&=\; 2(u_1v_2 - u_2v_1 - p_1q_2 + p_2q_1)\,, \end{aligned} \tag{16}$$

and the roots

$$\xi \;=\; \frac{h_0 - h_1 \pm \sqrt{h_1^2 - h_0h_2}}{h_0 - 2h_1 + h_2}\,. \tag{17}$$

Clearly the ERF has no inflections when $h_1^2 - h_0h_2 < 0$. When $h_1^2 - h_0h_2 > 0$, the ERF has no inflections or precisely one inflection on $\xi \in (0,1)$ according to whether the coefficients h_0, h_1, h_2 exhibit no sign changes or just one sign change; and if they exhibit two sign changes there may be either zero or two inflections for $\xi \in (0,1)$. A PH curve segment $\mathbf{r}(\xi)$, $\xi \in [\,0,1\,]$ is said to have a *monotone ERF* if its ERF has no inflections for $\xi \in (0,1)$.

Also of interest are the extrema of ω_1, which are identified by the roots of its arc–length derivative — namely,

$$\frac{\mathrm{d}\omega_1}{\mathrm{d}s} \;=\; 2\,\frac{\sigma(\xi)h'(\xi) - 2\,\sigma'(\xi)h(\xi)}{\sigma^4(\xi)}\,. \tag{18}$$

For a spatial PH quintic, the numerator of this expression is a polynomial of degree 5 in ξ (since $\sigma(\xi)$ and $h(\xi)$ are of degree 4 and 2), so ω_1 has at least 1 and at most 5 extrema, but not necessarily within $[\,0,1\,]$. Its coefficients can be determined from those of $h(\xi)$ and $\sigma(\xi)$ through standard algorithms [16] for the sums and products of polynomials in Bernstein form.

In the construction of rational MTFs from the ERF, it may be useful to subdivide the given PH quintic $\mathbf{r}(\xi)$ into subsegments with "simple" ERF variations, for which ω_1 is free of interior sign changes or extrema (or both). This may be accomplished by applying the de Casteljau algorithm [7] to the quaternion polynomial (4) at the roots of (9) or (18) on $\xi \in (0,1)$, if any — note that these subsegments will have matched ERFs at their junctures.

3 Minimal twist adapted frames

On a given space curve $\mathbf{r}(\xi)$, $\xi \in [\,0,1\,]$ of total arc length S, let

$$(\mathbf{f}_1(0), \mathbf{f}_2(0), \mathbf{f}_3(0)) \quad \text{and} \quad (\mathbf{f}_1(1), \mathbf{f}_2(1), \mathbf{f}_3(1)) \tag{19}$$

be the initial and final instances of an adapted frame $(\mathbf{f}_1(\xi), \mathbf{f}_2(\xi), \mathbf{f}_3(\xi))$ with $\mathbf{f}_1(\xi) = \mathbf{r}'(\xi)/|\mathbf{r}'(\xi)|$. If $\boldsymbol{\Omega} = \Omega_1\mathbf{f}_1 + \Omega_2\mathbf{f}_2 + \Omega_3\mathbf{f}_3$ is the angular velocity of this frame, it is called a *minimal twist frame* (MTF), subject to the boundary conditions (19), if (i) Ω_1 does not change sign for $\xi \in (0,1)$ — i.e., the frame is *monotone*; and (ii) it yields the least possible absolute value of the integral

$$T \;=\; \int_0^S \Omega_1 \,\mathrm{d}s \;=\; \int_0^1 \Omega_1(\xi)\;\sigma(\xi)\,\mathrm{d}\xi\,.$$

A point where Ω_1 changes sign is an *inflection* of the frame $(\mathbf{f}_1, \mathbf{f}_2, \mathbf{f}_3)$. In the absence of inflections, the values of T for different frames with the same end states can differ only by integer multiples of 2π. However, if inflections are present, the value of T will incorporate cancellation of clockwise and anti–clockwise rotations of $\mathbf{f}_2, \mathbf{f}_3$ about $\mathbf{f}_1$, a behavior that is inconsistent with the desired "minimal twist" property, and is excluded by stipulation (i).

Consider an adapted frame $(\mathbf{f}_1(\xi), \mathbf{f}_2(\xi), \mathbf{f}_3(\xi))$ on a PH space curve $\mathbf{r}(\xi)$, $\xi \in [\,0, 1\,]$ specified in terms of the ERF by $\mathbf{f}_1(\xi) = \mathbf{e}_1(\xi)$ and

$$\begin{bmatrix} \mathbf{f}_2(\xi) \\ \mathbf{f}_3(\xi) \end{bmatrix} \;=\; \begin{bmatrix} \cos\theta(\xi) & \sin\theta(\xi) \\ -\sin\theta(\xi) & \cos\theta(\xi) \end{bmatrix} \begin{bmatrix} \mathbf{e}_2(\xi) \\ \mathbf{e}_3(\xi) \end{bmatrix}, \tag{20}$$

which amounts to orienting $\mathbf{f}_2(\xi), \mathbf{f}_3(\xi)$ relative to $\mathbf{e}_2(\xi), \mathbf{e}_3(\xi)$ in the normal plane by the angular function $\theta(\xi)$. To obtain a *rational* frame, we choose

$$\theta(\xi) \;=\; 2\,\tan^{-1}\frac{b(\xi)}{a(\xi)}\,. \tag{21}$$

for relatively prime polynomials $a(\xi)$, $b(\xi)$ of given degree m, so that

$$\cos\theta(\xi) \;=\; \frac{a^2(\xi) - b^2(\xi)}{a^2(\xi) + b^2(\xi)}\,, \quad \sin\theta(\xi) \;=\; \frac{2\,a(\xi)b(\xi)}{a^2(\xi) + b^2(\xi)}\,. \tag{22}$$

Let $\boldsymbol{\Omega}$ be the angular velocity of the frame $(\mathbf{f}_1(\xi), \mathbf{f}_2(\xi), \mathbf{f}_3(\xi))$, with

$$\frac{\mathrm{d}\mathbf{f}_1}{\mathrm{d}s} \;=\; \boldsymbol{\Omega} \times \mathbf{f}_1\,, \qquad \frac{\mathrm{d}\mathbf{f}_2}{\mathrm{d}s} \;=\; \boldsymbol{\Omega} \times \mathbf{f}_2\,, \qquad \frac{\mathrm{d}\mathbf{f}_3}{\mathrm{d}s} \;=\; \boldsymbol{\Omega} \times \mathbf{f}_3\,.$$

Relative to the ERF (i.e., writing $\boldsymbol{\Omega} = \Omega_1\mathbf{e}_1 + \Omega_2\mathbf{e}_2 + \Omega_3\mathbf{e}_3$) it has components

$$\Omega_1(\xi) \;=\; \omega_1(\xi) + \frac{\theta'(\xi)}{\sigma(\xi)}\,, \tag{23}$$

and $\Omega_2(\xi) = \omega_2(\xi)$, $\Omega_3(\xi) = \omega_3(\xi)$, where from (21) we have

$$\theta'(\xi) \;=\; 2\,\frac{a(\xi)b'(\xi) - a'(\xi)b(\xi)}{a^2(\xi) + b^2(\xi)}\,. \tag{24}$$

The initial and final frames (19) are defined by specifying initial and final normal–plane orientations, $\theta_i = \theta(0)$ and $\theta_f = \theta(1)$, of $\mathbf{f}_2(\xi), \mathbf{f}_3(\xi)$ relative to $\mathbf{e}_2(\xi), \mathbf{e}_3(\xi)$ such that $\theta_i, \theta_f \in (-\pi, +\pi\,]$. However, the boundary conditions do not determine a unique adapted frame $(\mathbf{f}_1(\xi), \mathbf{f}_2(\xi), \mathbf{f}_3(\xi))$. The frame has the angular velocity component (23) in the tangent direction, where $\omega_1(\xi)$ is the angular velocity component of the ERF, and $\theta'(\xi)/\sigma(\xi)$ is the component incurred by the normal–plane rotation (20), so the choice of $\theta(\xi)$ influences the frame variation between the specified end states. In general, the twist of an adapted frame on a space curve, with given initial and final orientations,

may exceed 2π in magnitude, indicating a total rotation in exceess of what is necessary to satisfy the boundary conditions, by one or more full revolutions.

Now the twist of the frame $(\mathbf{f}_1, \mathbf{f}_2, \mathbf{f}_3)$ is given by

$$T \;=\; \int_0^S \Omega_1 \, \mathrm{d}s \;=\; \int_0^1 \omega_1 \sigma + \theta' \, \mathrm{d}\xi \;=\; T_{\mathrm{ERF}} + \theta_f - \theta_i \,, \tag{25}$$

and the magnitude of T may exceed 2π, since T_{ERF} may be greater than 2π in magnitude, and θ_i and θ_f are indeterminate up to integer multiples of 2π. Since an MTF can alway satisfy initial/final orientations with a total twist not less than $-\pi$ or greater than $+\pi$, the *reduced twist* $T_{\min}$ is used in lieu of the nominal value $T = \theta_f - \theta_i$. If $T \in (-\pi, +\pi\,]$ we take $T_{\min} = T$. Otherwise, we define $T_{\min}$ by adding to or subtracting from T the integer multiple of 2π that yields a value in the domain $(-\pi, +\pi\,]$.

A minimal twist frame, under given boundary conditions, is characterized by having the twist value $T_{\min}$, and the mean angular velocity component

$$\overline{\Omega}_1 \;=\; \frac{T_{\min}}{S} \,. \tag{26}$$

A closed–form expression for the frame vectors $\mathbf{f}_2(\xi)$ and $\mathbf{f}_3(\xi)$ that achieve the constant angular velocity component $\overline{\Omega}_1$ in the tangent direction $\mathbf{e}_1(\xi) = \mathbf{f}_1(\xi)$ is specified by (20) where, on setting $\Omega_1(\xi) \equiv \overline{\Omega}_1$ in (23) and integrating, the angle function $\theta(\xi)$ has the form

$$\theta(\xi) \;=\; \theta_i \;+\; \overline{\Omega}_1 \, s(\xi) \;-\; 2 \int_0^\xi \frac{h(x)}{\sigma(x)} \, \mathrm{d}x \,, \tag{27}$$

and the integral on the right admits the closed–form reduction (15). Figure 1 illustrates an example of a spatial PH quintic curve with specified initial/final orientations for the frame normal–plane vectors $\mathbf{f}_2(\xi)$ and $\mathbf{f}_3(\xi)$, and the exact MTF variation of these vectors along the curve, as defined by (20) and (27). Figure 2 compares the variation of the angular velocity component along the tangent direction for the ERF and MTF in this example.

4 Rational minimal twist frames

Expressions (20) and (27) define an MTF that satisfies the desirable constant angular velocity constraint $\Omega_1(\xi) \equiv \overline{\Omega}_1$, but this imposes a rather complicated

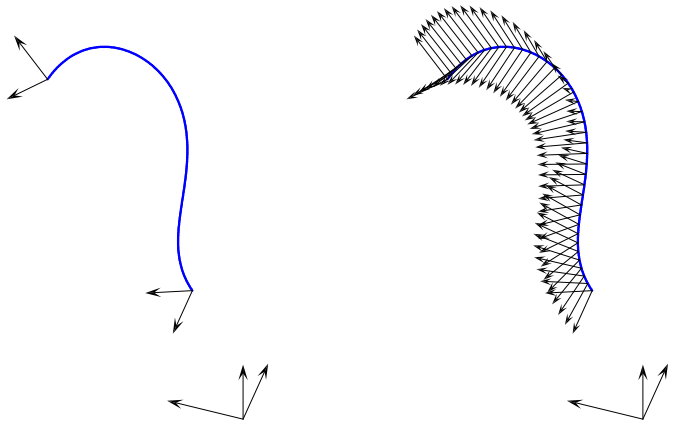

Figure 1: Left: A spatial PH quintic $\mathbf{r}(\xi)$ with given initial/final orientations $\mathbf{f}_2(0), \mathbf{f}_3(0)$ and $\mathbf{f}_2(1), \mathbf{f}_3(1)$ for the normal–plane vectors of an adapted frame $(\mathbf{f}_1(\xi), \mathbf{f}_2(\xi), \mathbf{f}_3(\xi))$. Right: the exact MTF variation of the vectors $\mathbf{f}_2(\xi), \mathbf{f}_3(\xi)$ along $\mathbf{r}(\xi)$, as specified by (20) and (27), subject to the boundary conditions.

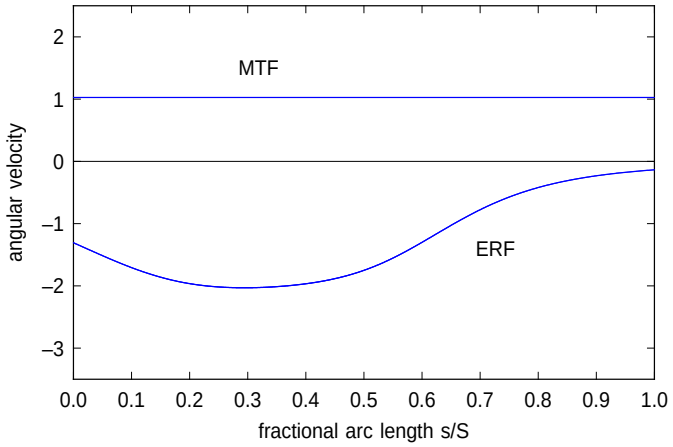

Figure 2: Variation with arc length of the frame angular velocity component in the tangent direction, for the Euler–Rodrigues frame (ERF) and minimal twist frame (MTF), along the spatial PH quintic example shown in Figure 1.

functional form on $\mathbf{f}_2(\xi)$ and $\mathbf{f}_3(\xi)$. Although $s(\xi)$ is a polynomial, the integral in (27) has a transcendental dependence on ξ, as seen in (15). Moreover, the sine and cosine of the expression (27) are required in (20).

In many applications, it is preferable to relax the constant angular velocity condition, in order to obtain an MTF with simpler (rational) expressions for the normal–plane vectors $\mathbf{f}_2(\xi), \mathbf{f}_3(\xi)$. Such a frame can be constructed from the form (21), for real polynomials $a(\xi)$ and $b(\xi)$. It is convenient to combine them into a complex polynomial $\mathbf{w}(\xi) = a(\xi) + \mathrm{i}\, b(\xi)$, such that

$$\exp(\mathrm{i}\,\theta(\xi)) \;=\; \frac{\mathbf{w}^2(\xi)}{|\mathbf{w}(\xi)|^2} \;=\; \frac{a^2(\xi) - b^2(\xi) + \mathrm{i}\, 2a(\xi)b(\xi)}{a^2(\xi) + b^2(\xi)}\,. \tag{28}$$

This can be more compactly formulated as

$$\exp(\mathrm{i}\,\theta(\xi)) \;=\; \mathbf{w}(\xi)/\overline{\mathbf{w}}(\xi)\,, \tag{29}$$

$\overline{\mathbf{w}}(\xi) = a(\xi) - \mathrm{i}\, b(\xi)$ being the conjugate of $\mathbf{w}(\xi)$, and equation (24) becomes

$$\theta'(\xi) \;=\; 2\,\frac{\mathrm{Im}(\overline{\mathbf{w}}(\xi)\mathbf{w}'(\xi))}{|\mathbf{w}(\xi)|^2} \;=\; 2\,\frac{a(\xi)b'(\xi) - a'(\xi)b(\xi)}{a^2(\xi) + b^2(\xi)}\,. \tag{30}$$

It should be noted that $\Omega_1 \equiv$ constant is never achieved when $\mathbf{f}_2(\xi), \mathbf{f}_3(\xi)$ are defined by (20) and (21). If $\deg(u, v, p, q) = m$ and $\deg(a, b) = l$, then

$$\deg(h) = 2m - 2,\ \deg(\sigma) = 2m,\ \deg(ab' - a'b) = 2l - 2,\ \deg(a^2 + b^2) = 2l.$$

Thus from (23) with $\omega_1 = 2h/\sigma^2$ and $\theta' = 2(ab' - a'b)/(a^2 + b^2)$, we obtain

$$\Omega_1 \;=\; 2\,\frac{(a^2 + b^2)h + \sigma(ab' - a'b)}{\sigma^2(a^2 + b^2)}\,, \tag{31}$$

and since this rational function has a numerator of degree $2m + 2l - 2$ and a denominator of degree $4m + 2l$, it cannot be a constant. Note that real roots of the numerator identify inflections of the frame $(\mathbf{f}_1(\xi), \mathbf{f}_2(\xi), \mathbf{f}_3(\xi))$.

Now when the polynomial $\mathbf{w}(\xi)$ is expressed in Bernstein form as

$$\mathbf{w}(\xi) \;=\; \sum_{k=0}^{m} \mathbf{w}_k \binom{m}{k} (1 - \xi)^{m-k} \xi^k\,, \tag{32}$$

the boundary constraints $\theta(0) = \theta_i$ and $\theta(1) = \theta_f$ yield the conditions

$$\mathbf{w}_0/\overline{\mathbf{w}}_0 \;=\; \exp(\mathrm{i}\,\theta_i) \quad \text{and} \quad \mathbf{w}_m/\overline{\mathbf{w}}_m \;=\; \exp(\mathrm{i}\,\theta_f)\,,$$

and hence $\mathbf{w}_0 = \gamma_i \exp(\mathrm{i}\frac{1}{2}\theta_i)$, $\mathbf{w}_m = \gamma_f \exp(\mathrm{i}\frac{1}{2}\theta_f)$ for non–zero real constants γ_i, γ_f. However, since expression (29) remains unchanged on scaling $\mathbf{w}(\xi)$ by any non–zero real value, we can set $\gamma_i = 1$ or $\gamma_f = 1$. Henceforth, we take

$$\mathbf{w}_0 \;=\; \exp(\mathrm{i}\tfrac{1}{2}\theta_i) \quad \text{and} \quad \mathbf{w}_m \;=\; \gamma\, \exp(\mathrm{i}\tfrac{1}{2}\theta_f)\,.$$

It is preferable to maintain $\mathbf{w}(\xi) = a(\xi) + \mathrm{i}\, b(\xi)$ of low degree, so $\mathbf{f}_2(\xi), \mathbf{f}_3(\xi)$ as defined by (20) are of reasonable degree. We begin by dispensing with the case of a linear $\mathbf{w}(\xi)$, and then treat in detail the case of a quadratic $\mathbf{w}(\xi)$.

4.1 Linear polynomial $\mathbf{w}(\xi)$

In the simplest non–trivial case ($m = 1$), setting

$$\mathbf{w}(\xi) \;=\; \mathbf{w}_0(1-\xi) + \mathbf{w}_1\xi$$

with $\mathbf{w}_0 = \exp(\mathrm{i}\frac{1}{2}\theta_i)$ and $\mathbf{w}_1 = \gamma\, \exp(\mathrm{i}\frac{1}{2}\theta_f)$, the expression (30) becomes

$$\theta'(\xi) \;=\; \frac{2\,\gamma\, \sin\frac{1}{2}\Delta\theta}{(1-\xi)^2 + \gamma\, \cos\frac{1}{2}\Delta\theta\, 2(1-\xi)\xi + \gamma^2\xi^2}\,,$$

where $\Delta\theta = \theta_f - \theta_i$. Since the numerator is a constant, and the denominator is quadratic with discriminant $-\,(\gamma\, \sin\frac{1}{2}\Delta\theta)^2$, we note that θ' cannot change sign, so $\theta(\xi)$ is monotone, with $\theta(\xi) \equiv 0$ when $\theta_f = \theta_i$. The quantity γ is the only parameter available to modulate the variation of $\theta(\xi)$. Setting

$$\rho_0 \;=\; \sigma(0)\,[\,\overline{\Omega}_1 - \omega_1(0)\,] \qquad \text{and} \qquad \rho_1 \;=\; \sigma(1)\,[\,\overline{\Omega}_1 - \omega_1(1)\,]\,, \tag{33}$$

one can verify that the choices

$$\gamma \;=\; \frac{\rho_0}{2\,\sin\frac{1}{2}\Delta\theta} \qquad \text{and} \qquad \gamma \;=\; \frac{2\,\sin\frac{1}{2}\Delta\theta}{\rho_1}$$

yield $\Omega_1(0) = \overline{\Omega}_1$ and $\Omega_1(1) = \overline{\Omega}_1$, respectively. Agreement of $\Omega_1(\xi)$ with the value (26) can thus be achieved at only one end point. The case of a linear $\mathbf{w}(\xi)$ evidently offers insufficient scope for modulating the variation of $\Omega_1(\xi)$.

4.2 Quadratic polynomial $\mathbf{w}(\xi)$

In the case of a quadratic polynomial,

$$\mathbf{w}(\xi) \;=\; \mathbf{w}_0(1-\xi)^2 + \mathbf{w}_1 2(1-\xi)\xi + \mathbf{w}_2\xi^2\,, \tag{34}$$

the numerator of (30) is quadratic and the denominator is quartic. For $\mathbf{w}(\xi)$ quadratic, the MTF vectors on a spatial PH quintic obtained from (20) have a rational dependence of degree 8 on the curve parameter ξ.

Choosing $\mathbf{w}_0 = \exp(\mathrm{i}\frac{1}{2}\theta_i)$ and $\mathbf{w}_2 = \gamma\,\exp(\mathrm{i}\frac{1}{2}\theta_f)$, and using the quantities (33), one can verify that the choice

$$\mathbf{w}_1 \;=\; \frac{\exp(\mathrm{i}\frac{1}{2}\theta_f)\,\rho_0 + \exp(\mathrm{i}\frac{1}{2}\theta_i)\,\gamma\,\rho_1}{4\sin\frac{1}{2}\Delta\theta} \tag{35}$$

yields $\Omega_1(0) = \Omega_1(1) = \overline{\Omega}_1$, so $\Omega_1(\xi)$ agrees with the value (26) at both end points, and γ remains as a free parameter. Using (35), the numerator of (30) has the Bernstein coefficients

$$2\,\mathrm{Im}(\overline{\mathbf{w}}_0\mathbf{w}_1) = \tfrac{1}{2}\,\rho_0\,,\;\; 2\,\mathrm{Im}(\overline{\mathbf{w}}_0\mathbf{w}_2) = 2\,\gamma\sin\tfrac{1}{2}\Delta\theta\,,\;\; 2\,\mathrm{Im}(\overline{\mathbf{w}}_1\mathbf{w}_2) = \tfrac{1}{2}\,\gamma^2\rho_1\,,$$

and the Bernstein coefficients of the denominator are

$$\begin{aligned}
|\mathbf{w}_0|^2 \;&=\; 1\,,\\
2\,\mathrm{Re}(\overline{\mathbf{w}}_0\mathbf{w}_1) \;&=\; \frac{\cos\frac{1}{2}\Delta\theta\,\rho_0 + \gamma\,\rho_1}{2\sin\frac{1}{2}\Delta\theta}\,,\\
2\,\mathrm{Re}(\overline{\mathbf{w}}_0\mathbf{w}_2) + 4\,|\mathbf{w}_1|^2 \;&=\; \frac{\rho_0^2 + 2\,\gamma\cos\frac{1}{2}\Delta\theta\,\rho_0\rho_1 + \gamma^2\rho_1^2}{16\sin^2\frac{1}{2}\Delta\theta}\,,\\
2\,\mathrm{Re}(\overline{\mathbf{w}}_1\mathbf{w}_2) \;&=\; \frac{\rho_0 + \gamma^2\cos\frac{1}{2}\Delta\theta\,\rho_1}{2\sin\frac{1}{2}\Delta\theta}\,,\\
|\mathbf{w}_2|^2 \;&=\; \gamma^2\,.
\end{aligned}$$

To fix the free parameter γ, we consider minimization of the mean square deviation of $\Omega_1(\xi)$ from the average value $\overline{\Omega}_1$, as defined by

$$\langle\,|\Delta\Omega_1|^2\,\rangle \;=\; \frac{1}{S}\int_0^1 [\,\Omega_1(\xi) - \overline{\Omega}_1\,]^2\;\sigma(\xi)\,\mathrm{d}\xi\,. \tag{36}$$

On expanding the integrand and noting that

$$\int_0^1 \Omega_1(\xi)\;\sigma(\xi)\,\mathrm{d}\xi \;=\; S\,\overline{\Omega}_1\,,$$

the expression (36) can be reduced to

$$\langle\, |\Delta\Omega_1|^2 \,\rangle \;=\; \frac{1}{S}\int_0^1 \Omega_1^2(\xi)\,\sigma(\xi)\,\mathrm{d}\xi \;-\; \overline{\Omega}_1^2\,.$$

Thus, using (23) and noting that $\overline{\Omega}_1$ is a constant, $\langle\, |\Delta\Omega_1|^2 \,\rangle$ can be minimized with respect to the parameter γ by determining the minima of the integral

$$F(\gamma) \;=\; \int_0^1 \left[\,\omega_1(\xi) + \frac{\theta'(\xi)}{\sigma(\xi)}\,\right]^2 \sigma(\xi)\,\mathrm{d}\xi\,, \tag{37}$$

where only $\theta'(\xi)$ depends on γ. The extrema of (36) satisfy the condition

$$\frac{\mathrm{d}F}{\mathrm{d}\gamma} \;=\; 2\int_0^1 \left[\,\omega_1(\xi) + \frac{\theta'(\xi)}{\sigma(\xi)}\,\right] \frac{\partial\theta'}{\partial\gamma}(\xi)\,\sigma(\xi)\,\mathrm{d}\xi \;=\; 0\,.$$

The above integral is, in principle, amenable to closed–form reduction, since the polynomials appearing in it are of degree 4 at most. However, upon taking the partial derivative of $\theta'(\xi)$ with respect to γ, this reduction becomes very cumbersome, and in general the resulting equation will have a transcendental dependence on γ that necessitates an iterative numerical solution.

Instead, we use the following approach. For $\gamma \neq 0$, the function[2] (37) can be computed to any desired precision through the Simpson quadrature rule [28]. For uniform nodes $\xi_i = i/N$, $i = 0, \ldots, N$ (with N even) this estimates the integral (37) as

$$F(\gamma) \;\approx\; \frac{1}{3N}\sum_{i=1}^{N/2} f(\xi_{2i-2}) + 4\,f(\xi_{2i-1}) + f(\xi_{2i})\,, \tag{38}$$

where $f(\xi) = \Omega_1^2(\xi)\,\sigma(\xi)$. Choosing $N = 2^n$ for $n = 1, 2, \ldots$, the previously–computed f values can be re–used upon increasing n to $n+1$. Since $f(\xi)$ is non–negative, this yields rapid convergence to any desired tolerance. It can be shown that the error ϵ in the estimate (38) satisfies

$$|\epsilon| \;<\; \frac{1}{180N^4}\max_{\xi\in[0,1]} |f^{(4)}(\xi)|\,.$$

[2]The value $\gamma = 0$ is excluded, since then $\mathbf{w}_2 = 0$ and by l'Hôpital's rule the limiting value of (29) as $\xi \to 1$ fails to yield interpolation of the specified frame vectors $\mathbf{f}_2(1), \mathbf{f}_3(1)$.

Combining the ability to efficiently compute $F(\gamma)$ to any prescribed accuracy with a simple scheme [3] for minimization of a univariate function over a given interval in γ, without the need for derivative information, yields the rational MTF whose angular velocity component $\Omega_1(\xi)$ most closely agrees with the constant mean value $\overline{\Omega}_1$, when the complex polynomial $\mathbf{w}(\xi) = a(\xi) + \mathrm{i}\, b(\xi)$, which defines the "compensating" ERF rotation (20), is quadratic.

4.3 Refinement by subdivision

As emphasized in Section 3, an MTF $(\mathbf{f}_1, \mathbf{f}_2, \mathbf{f}_3)$ must not exhibit sign changes in the angular velocity component Ω_1, since a cancellation of clockwise and anti–clockwise rotation of $\mathbf{f}_2$ and $\mathbf{f}_3$ about $\mathbf{f}_1$ is inconsistent with the desired "minimal twist" property of such frames. Because of the non–linear nature of the construction, the imposition of this requirement as an *a priori* constraint is a challenging task. However, it is not difficult to check *a posteriori* whether it has been satisfied — and, if not, implement corrective measures.

The frame angular velocity component $\Omega_1(\xi)$ can be expressed in the form (31) in terms of the parametric speed (3), the polynomial (9), and the real and imaginary parts of the complex polynomial $\mathbf{w}(\xi) = a(\xi) + \mathrm{i}\, b(\xi)$. For a quintic PH curve and quadratic $\mathbf{w}(\xi)$, the numerator of (31) is a polynomial of degree 6 whose Bernstein coefficients can be computed by standard algorithms [16]. The subdivision and variation–diminishing properties can then be invoked to identify its real roots, if any, on the domain $\xi \in (0, 1)$.

Failure of frame monotonicity in computing a rational MTF is generally a consequence of the inadequacy of the sole free parameter γ to compensate for variation in the ERF angular velocity ω_1 over the entire curve $\mathbf{r}(\xi)$, $\xi \in [\,0, 1\,]$. To remedy this, the domain $[\,0, 1\,]$ can be decomposed into subsets over which the ERF exhibits "simple" behavior. Two types of subdivision points were identified in Section 2.2 — (i) the roots of (9) where ω_1 changes sign; and (ii) the roots of the numerator of (18) where ω_1 is extremal. The points (i) and (ii) identify subintervals over which ω_1 does not change sign, and is monotone increasing or decreasing, respectively. The simpler behavior of ω_1 over the subintervals delineated by either (or both) of these point sets makes it much easier for the normal–plane rotation (20) specified by the complex quadratic polynomial $\mathbf{w}(\xi) = a(\xi) + \mathrm{i}\, b(\xi)$ to compensate for its variation.

Suppose that N subdivision points $\xi_1, \ldots, \xi_N \in (0, 1)$ are identified. With $\xi_0 = 0$ and $\xi_{N+1} = 1$, they define $N + 1$ parameter subintervals $[\,\xi_{k-1}, \xi_k\,]$ as domains for subsegments of $\mathbf{r}(\xi)$ with the arc lengths $\Delta S_k = s(\xi_k) - s(\xi_{k-1})$,

$k = 1, \ldots, N+1$. A portion T_k of the reduced twist $T_{\min}$ for the entire curve is assigned to each of these subsegments, according to

$$T_k \;=\; \frac{\Delta S_k}{S}\, T_{\min}\,. \tag{39}$$

Setting $\theta_0 = \theta_i$ and $\theta_{N+1} = \theta_f$, a set of intermediate orientations $\theta_1, \ldots, \theta_N$ of the MTF vectors $\mathbf{f}_2(\xi), \mathbf{f}_3(\xi)$ relative to the ERF vectors $\mathbf{e}_2(\xi), \mathbf{e}_3(\xi)$ at the points $\xi_1, \ldots, \xi_N$ must be assigned. Let $\theta(\xi)$ specify the continuous rotation (20) of $\mathbf{e}_2(\xi), \mathbf{e}_3(\xi)$ onto $\mathbf{f}_2(\xi), \mathbf{f}_3(\xi)$. Then, from (10) and (23), we must have

$$\int_{\xi_{k-1}}^{\xi_k} \left[\, 2\,\frac{h(\xi)}{\sigma^2(\xi)} + \frac{\theta'(\xi)}{\sigma(\xi)} \,\right] \sigma(\xi)\,\mathrm{d}\xi \;=\; T_k\,,$$

in order for the subsegment $\xi \in [\,\xi_{k-1}, \xi_k\,]$ to have the twist value (39). This condition reduces to

$$\theta(\xi_k) \;=\; \theta(\xi_{k-1}) \;+\; T_k - T_{\mathrm{ERF},\,k}\,, \tag{40}$$

where

$$T_{\mathrm{ERF},\,k} \;=\; 2\int_{\xi_{k-1}}^{\xi_k} \frac{h(\xi)}{\sigma(\xi)}\,\mathrm{d}\xi \tag{41}$$

is the total ERF twist for subsegment k, which may be determined as twice the difference of expression (15), evaluated at $\xi = \xi_k$ and $\xi = \xi_{k-1}$.

The relation (40) recursively defines a sequence $\theta_1, \ldots, \theta_N$ of intermediate orientations of the MTF relative to the ERF, in terms of the known quantities (39) and (41), upon setting $\theta_k = \theta(\xi_k)$ for $k = 1, \ldots, N$. With these values, we can specify boundary conditions for "local" angular functions $\theta_k(\xi)$, $\xi \in [\,\xi_{k-1}, \xi_k\,]$ on each subsegment by choosing $\theta_k(0) = \theta_{k-1}$ and $\theta_k(1) = \theta_k$. These functions are defined through the relations

$$\exp(\mathrm{i}\,\theta_k(\xi)) \;=\; \mathbf{w}_k(\xi)/\overline{\mathbf{w}}_k(\xi)\,,$$

where $\mathbf{w}_k(\xi)$ is a complex quadratic polynomial associated with subsegment k, expressed in Bernstein form on the interval $\xi \in [\,\xi_{k-1}, \xi_k\,]$ as

$$\mathbf{w}_k(\xi) \;=\; \frac{\mathbf{w}_{k,0}(\xi_k - \xi)^2 + \mathbf{w}_{k,1} 2(\xi_k - \xi)(\xi - \xi_{k-1}) + \mathbf{w}_{k,2}(\xi - \xi_{k-1})^2}{(\Delta\xi_k)^2}\,,$$

where $\Delta\xi_k = \xi_k - \xi_{k-1}$. By analogy with the arguments used in Section 4.2, we use the values $\mathbf{w}_{k,0} = \exp(\mathrm{i}\frac{1}{2}\theta_{k-1})$, $\mathbf{w}_{k,2} = \gamma_k \exp(\mathrm{i}\frac{1}{2}\theta_k)$, and

$$\mathbf{w}_{k,1} \;=\; \frac{\exp(\mathrm{i}\frac{1}{2}\theta_k)\,\rho_{k-1} + \exp(\mathrm{i}\frac{1}{2}\theta_{k-1})\,\gamma_k\rho_k}{4\sin\frac{1}{2}\Delta\theta_k}\,\Delta\xi_k\,,$$

where $\Delta\theta_k = \theta_k - \theta_{k-1}$ and

$$\rho_{k-1} \;=\; \sigma(\xi_{k-1})\,[\,\overline{\Omega}_1 - \omega_1(\xi_{k-1})\,]\,, \quad \rho_k \;=\; \sigma(\xi_k)\,[\,\overline{\Omega}_1 - \omega_1(\xi_k)\,]\,.$$

The free parameters γ_k are individually determined for each subsegment k by minimizing the integral (37), restricted to the domain $\xi \in [\,\xi_{k-1}, \xi_k\,]$.

Note that the MTF frames obtained through this subdivision scheme are continuous in orientation and its first derivative (angular velocity), but not second derivative (angular acceleration). However, since the rms variation of the angular velocity Ω_1 about the mean value $\overline{\Omega}_1$ is greatly suppressed when using this subdivision scheme (see Example 3 below), the discontinuities in angular acceleration are typically insignificant.

5 Algorithm and computed examples

To assist in implementation, the preceding analysis is now summarized in an algorithm outline, and some computed examples are presented to illustrate representative results obtained from the algorithm. For brevity, the algorithm addresses only the core rational MTF construction based upon the quadratic complex polynomial (34), as described in Section 4.2. This can be coded as a basic function, to be called repeatedly with appropriate input parameters, when invoking the subdivision scheme described in Section 4.3 to adequately suppress variations in Ω_1 or to ensure monotonicity of the MTF.

Algorithm

input: spatial PH quintic $\mathbf{r}(\xi)$ with pre–image quaternion polynomial $\mathcal{A}(\xi)$ and orientations θ_i, θ_f of the initial and final frames (19) relative to the ERF.

1. compute the complex conjugate roots $\mathbf{z}_1, \overline{\mathbf{z}}_1$ and $\mathbf{z}_2, \overline{\mathbf{z}}_2$ of the parametric speed polynomial (3) and the corresponding residues (14);

2. compute the ERF twist T_{ERF} by taking the difference of expression (15) evaluated at $\xi = 1$ and $\xi = 0$;

3. define the reduced twist $T_{\min}$ by adding to or subtracting from (25) the integer multiple of 2π that yields a value $T_{\min} \in (-\pi, +\pi\,]$;

4. compute the mean angular velocity component $\overline{\Omega}_1$ defined by (26);

5. with γ a free parameter, set $\mathbf{w}_0 = \exp(\mathrm{i}\frac{1}{2}\theta_i)$ and $\mathbf{w}_2 = \gamma \exp(\mathrm{i}\frac{1}{2}\theta_f)$, and assign $\mathbf{w}_1$ according to expressions (33) and (35);

6. with the coefficients $\mathbf{w}_0, \mathbf{w}_1, \mathbf{w}_2$ express $\theta'(\xi)$ in terms of (34) using (30);

7. using an adaptive quadrature rule to evaluate (37), and a minimization scheme that does not employ derivatives, obtain the γ value that yields the least value for this integral;

8. instantiate $\mathbf{w}(\xi)$ by computing $\mathbf{w}_0, \mathbf{w}_1, \mathbf{w}_2$ for this γ value, and hence obtain the rational functions $\cos\theta(\xi)$ and $\sin\theta(\xi)$ from (22);

9. obtain the rational MTF frame vectors $\mathbf{f}_2(\xi), \mathbf{f}_3(\xi)$ from the ERF frame vectors $\mathbf{e}_2(\xi), \mathbf{e}_3(\xi)$ using (20) and set $\mathbf{f}_1(\xi) = \mathbf{e}_1(\xi)$.

output: rational MTF $(\mathbf{f}_1(\xi), \mathbf{f}_2(\xi), \mathbf{f}_3(\xi))$ on the PH quintic $\mathbf{r}(\xi)$ satisfying the specified boundary conditions, with minimized variation of the tangent–direction angular velocity component Ω_1 about the mean value $\overline{\Omega}_1$.

Example 1. The spatial PH quintic in Figure 1 is defined by the coefficients

$$\begin{aligned}
\mathcal{A}_0 &= -0.9515 + 0.9515\,\mathbf{i} + 0.3941\,\mathbf{j} - 0.3941\,\mathbf{k}\,, \\
\mathcal{A}_1 &= -0.2085 + 1.4435\,\mathbf{i} - 0.2981\,\mathbf{j} + 1.0472\,\mathbf{k}\,, \\
\mathcal{A}_2 &= 1.2294 + 0.6264\,\mathbf{i} + 1.3768\,\mathbf{j} - 0.0915\,\mathbf{k}\,.
\end{aligned}$$

Relative to the ERF, the orientations of the two end frames (19) are specified by the angles $\theta_i = 0.125\,\pi$ and $\theta_f = 0.50\,\pi$. For this curve, the ERF exhibits no inflections, since the Bernstein coefficients (16) are all negative. The total twist (25) is $T \approx -4.3703$, and the reduced twist is $T_{\min} \approx 1.9129$. Figure 3 illustrates the relative root–mean–square (rms) variation $\sqrt{\langle\, |\Delta\Omega_1|^2 \,\rangle}\,/\,|\overline{\Omega}_1|$ of Ω_1 about $\overline{\Omega}_1$ for $\gamma \in [\,-2, +2\,]$ with a neighborhood of $\gamma = 0$ excluded — the minimum is approximately 0.168, and occurs at $\gamma \approx -0.938$.

For this γ value, Figure 4 shows the angular velocity components $\omega_1(\xi)$ of the ERF, $\theta'(\xi)/\sigma(\xi)$ associated with the normal plane rotation (20)–(21), and $\Omega_1(\xi)$ of the rational MTF generated from (20). The angle function $\theta(\xi)$

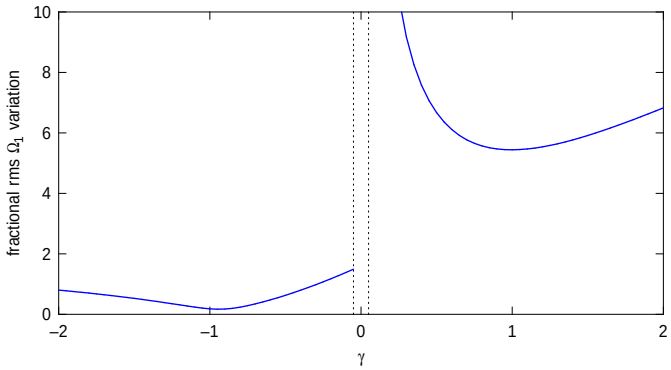

Figure 3: The dependence of the relative root–mean–square variation in the angular velocity component Ω_1, defined in terms of expressions (26) and (36) as $\sqrt{\langle\, |\Delta\Omega_1|^2 \,\rangle}\,/\,|\overline{\Omega}_1|$, on the parameter γ for the PH quintic in Example 1.

specified by (29) and (34) evidently performs very well in compensating for the ERF variation, so as to yield an MTF angular velocity component $\Omega_1(\xi)$ that conforms quite closely to the "ideal" constant value $\overline{\Omega}_1$.

For the optimum γ value, Figure 5 compares the variation of the normal plane vectors for the ERF and the rational MTF. For this comparison, the initial ERF vectors $\mathbf{e}_2(0), \mathbf{e}_3(0)$ are made to coincide with $\mathbf{f}_2(0), \mathbf{f}_3(0)$ by post–multiplying (4) with the unit quaternion $\mathcal{U} = \cos\frac{1}{2}\theta_i + \sin\frac{1}{2}\theta_i\,\mathbf{i}$. Comparing Figures 1 and Figure 5, it is apparent that the small variation in the angular velocity component Ω_1 of the rational MTF is barely discernible.

This example highlights the importance of the chosen γ value: it is evident from Figure 3 that positive γ values will generally yield poor results. Figure 6 shows the angular velocity components illustrated in Figure 4 again, but with $\gamma = 1$ (note the difference in the vertical scales). This value incurs a distinctly bimodal variation of $\theta'(\xi)/\sigma(\xi)$ which, because of the mild variation of $\omega_1(\xi)$, is mirrored in $\Omega_1(\xi)$. In fact $(\mathbf{f}_1(\xi), \mathbf{f}_2(\xi), \mathbf{f}_3(\xi))$ is no longer a true MTF, since $\Omega_1(\xi)$ changes sign and the total twist exceeds $T_{\min}$ by 2π.

Example 2. Consider next the spatial PH quintic defined by the coefficients

$$\begin{aligned}
\mathcal{A}_0 &= -1.3777 + 1.3777\,\mathbf{i} - 0.5444\,\mathbf{j} + 0.0000\,\mathbf{k}\,,\\
\mathcal{A}_1 &= -0.3078 + 0.9131\,\mathbf{i} + 1.1730\,\mathbf{j} + 1.9514\,\mathbf{k}\,,\\
\mathcal{A}_2 &= 1.7882 + 0.9111\,\mathbf{i} + 0.6158\,\mathbf{j} + 0.3853\,\mathbf{k}\,.
\end{aligned}$$

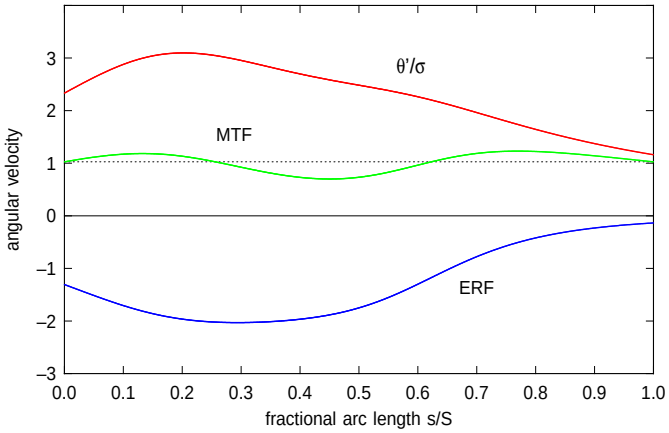

Figure 4: Angular velocity components in the tangent direction for the Euler–Rodrigues frame (ERF), the normal–plane rotation specified by (20)–(21), and the rational miminal twist frame (MTF) defined by (20) for $\gamma \approx -0.938$, the value that minimizes (36). The dashed line indicates the mean value $\overline{\Omega}_1$.

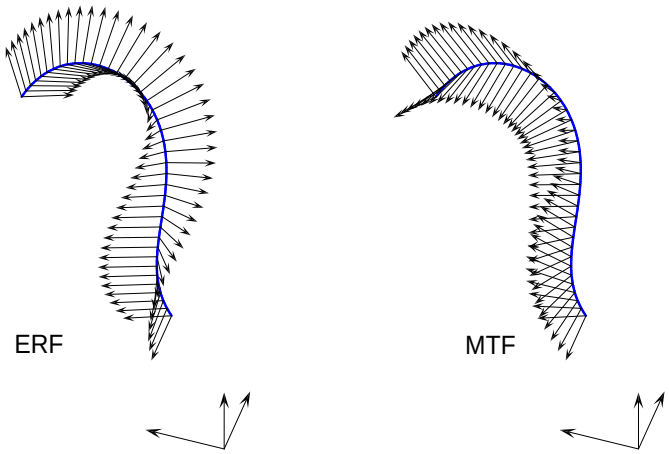

Figure 5: Comparison of normal–plane vectors of the Euler–Rodrigues frame (left) and the minimal twist frame (right) along the spatial PH quintic curve in Example 1. The initial orientations of the ERF and MTF are coincident.

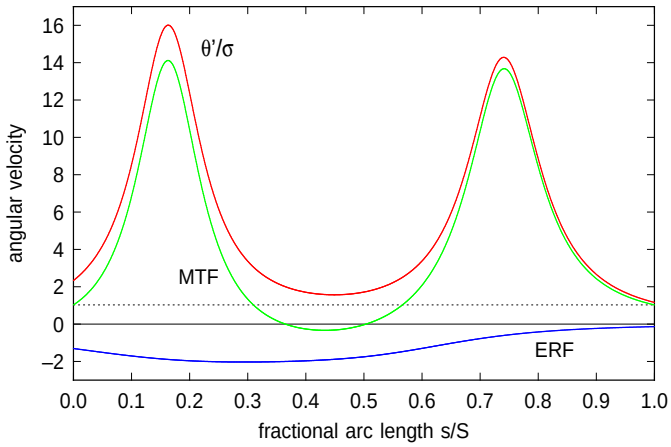

Figure 6: Angular velocity components in the tangent direction for the Euler–Rodrigues frame, normal–plane rotation specified by (20)–(21), and rational miminal twist frame defined by (20) for the "poor" choice $\gamma = 1$ used in (35).

The orientations of the two end frames (19) are specified by the angles $\theta_i = -1.25\,\pi$ and $\theta_f = 0.75\,\pi$, and the ERF has one inflection in this case. The total twist is $T \approx -3.6675$, and the reduced twist is $T_{\min} \approx 2.6157$. Figure 7 shows the dependence of the relative rms variation of Ω_1 about $\overline{\Omega}_1$ for $\gamma \in [-2, +2]$. The minimum value is approximately 0.112, at $\gamma \approx -0.749$.

For the optimum γ, Figure 8 shows the angular velocity components for the ERF, the rational normal plane rotation applied to it, and the resulting rational MTF. Again, the angle function $\theta(\xi)$ performs well in compensating for the ERF variation to yield a nearly–constant MTF angular velocity Ω_1. Figure 9 compares the ERF and MTF normal plane vectors along the curve: $\mathbf{e}_2(0), \mathbf{e}_3(0)$ are again made coincident with $\mathbf{f}_2(0), \mathbf{f}_3(0)$.

Example 3. Consider the spatial PH quintic defined by the coefficients

$$\begin{aligned}
\mathcal{A}_0 &= -1.2403 + 1.2403\,\mathbf{i} + 0.5039\,\mathbf{j} + 0.9070\,\mathbf{k}\,, \\
\mathcal{A}_1 &= -0.2745 + 0.6921\,\mathbf{i} + 1.5422\,\mathbf{j} - 1.1255\,\mathbf{k}\,, \\
\mathcal{A}_2 &= 1.6063 + 0.8184\,\mathbf{i} - 0.6131\,\mathbf{j} + 0.9349\,\mathbf{k}\,.
\end{aligned}$$

The orientations of the two end frames (19) are specified by the angles $\theta_i = -0.25\,\pi$ and $\theta_f = 1.25\,\pi$, and the ERF has one inflection in this case. The

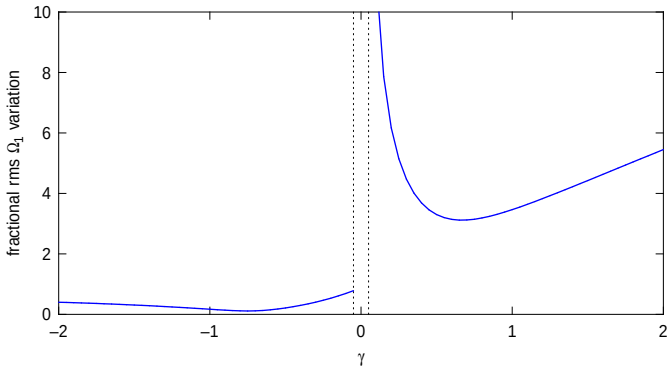

Figure 7: Variation of the relative root–mean–square variation in the angular velocity Ω_1 with the parameter γ for the spatial PH quintic in Example 2.

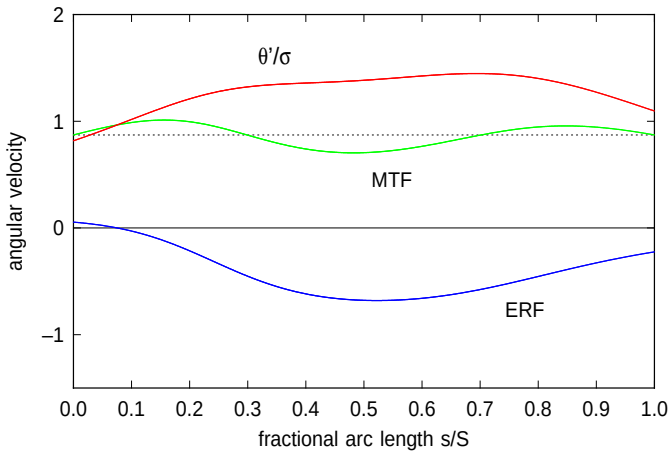

Figure 8: Angular velocity components in the tangent direction for the Euler–Rodrigues frame (ERF), the normal–plane rotation specified by (20)–(21), and rational miminal twist frame (MTF) defined by (20) with $\gamma \approx -0.749$, the value that minimizes (36). The dashed line indicates the mean value $\overline{\Omega}_1$.

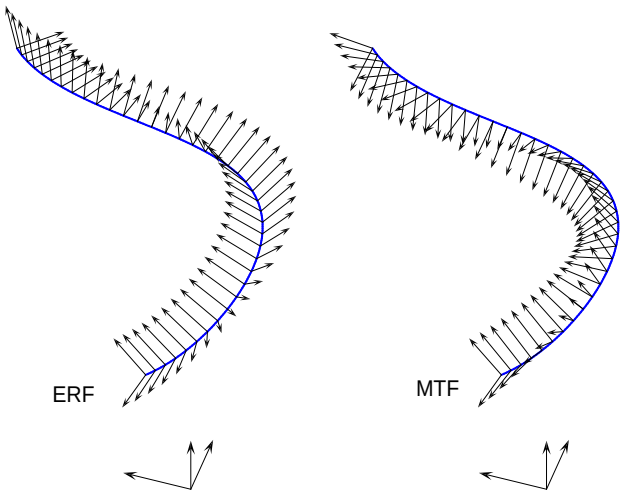

Figure 9: Comparison of normal–plane vectors of the Euler–Rodrigues frame (left) and the minimal twist frame (right) along the spatial PH quintic curve in Example 2. The initial ERF and MTF orientations are coincident.

total twist is $T \approx 2.2046$, and the reduced twist is $T_{\min} \approx 2.2046$. Figure 10 shows the dependence of the relative rms variation of Ω_1 about $\overline{\Omega}_1$ for $\gamma \in [-2, +2]$. The minimum value is approximately 0.555, at $\gamma \approx 0.557$.

For the optimum γ, Figure 11 shows the angular velocity components for the ERF, the rational normal plane rotation applied to it, and the rational frame $(\mathbf{f}_1(\xi), \mathbf{f}_2(\xi), \mathbf{f}_3(\xi))$. The ERF angular velocity component ω_1 exhibits a pronounced variation, with an inflection at $\xi \approx 0.2363$, a mild extremum at $\xi \approx 0.043205$, and a sharp extremum at $\xi \approx 0.6735$. Consequently, even with the optimum γ value, the angle function $\theta(\xi)$ cannot adequately compensate for this variation to achieve a nearly–constant MTF angular velocity Ω_1. As seen in Figure 11, the frame $(\mathbf{f}_1(\xi), \mathbf{f}_2(\xi), \mathbf{f}_3(\xi))$ exhibits two inflections, where Ω_1 changes sign, inconsistent with the definition of an MTF.

Figure 12 illustrates the dramatic improvement in the behavior of Ω_1 that can be achieved by a single subdivision, at the parameter value $\xi_m \approx 0.6735$ identifying the sharp extremum in the ERF angular velocity ω_1. Individual optimum values $\gamma_1 \approx 1.351$ and $\gamma_2 \approx 0.563$ were identified for the segments $\xi \in [0, \xi_m]$ and $\xi \in [\xi_m, 1]$ yielding fractional rms deviations of Ω_1 about $\overline{\Omega}_1$ of 0.0138 and 0.0471. It can be seen that the inflections of the rational frame

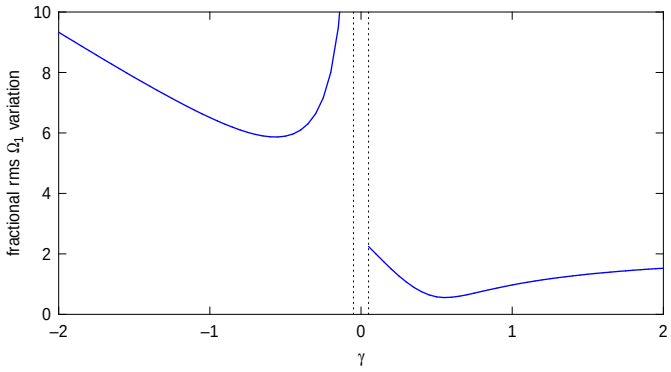

Figure 10: Variation of relative root–mean–square variation in the angular velocity Ω_1 with the parameter γ for the spatial PH quintic in Example 3.

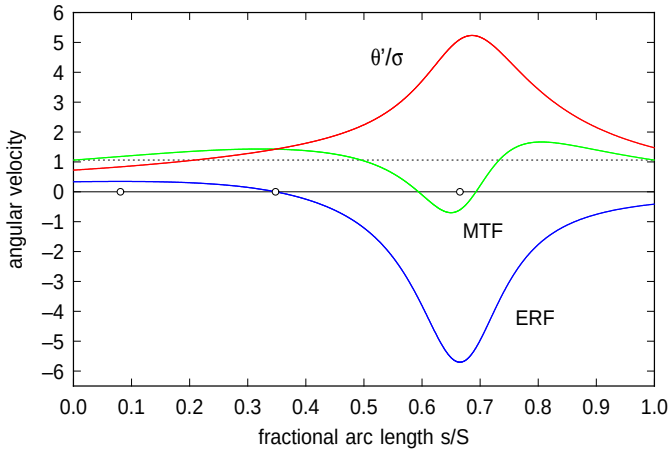

Figure 11: Angular velocity components on the curve in Example 3, for the value $\gamma \approx 0.557$ minimizing (36). In this case, the ERF angular velocity ω_1 has one inflection and two extrema (identified by dots on the horizontal axis) and the frame $(\mathbf{f}_1(\xi), \mathbf{f}_2(\xi), \mathbf{f}_3(\xi))$ is not a true MTF because Ω_1 changes sign.

$(\mathbf{f}_1(\xi), \mathbf{f}_2(\xi), \mathbf{f}_3(\xi))$ evident in Figure 11 have been eliminated, and the MTF angular velocity Ω_1 adheres very closely to the mean value $\overline{\Omega}_1$ (the deviation may be further suppressed, if desired, through further subdivision).

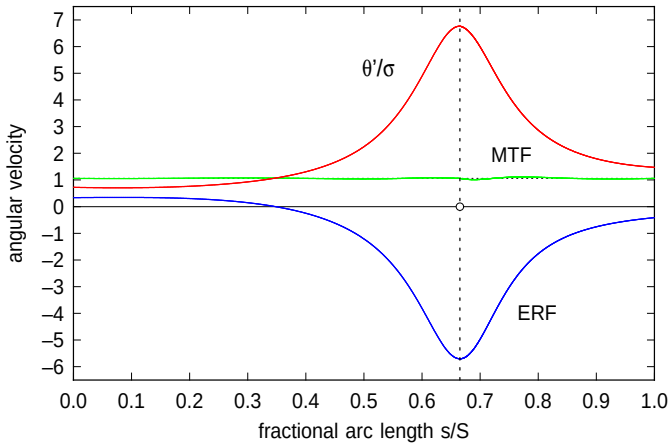

Figure 12: Angular velocity components in Example 3 after subdivision at the ERF angular velocity extremum, indicated by the dashed line. The two curve segments have the individual optimum values $\gamma_1 \approx 1.351$, $\gamma_2 \approx 0.563$. Comparison with Figure 11 shows that the rational rotations (20) now yield a true MTF, with Ω_1 exhibiting only minor deviations about the mean $\overline{\Omega}_1$.

Figure 13 compares the ERF and MTF normal plane vectors along the curve after subdivision at the sharp extremum in the ERF angular velocity component ω_1, with $\mathbf{e}_2(0), \mathbf{e}_3(0)$ again made coincident with $\mathbf{f}_2(0), \mathbf{f}_3(0)$. Note the rapid twisting of $\mathbf{e}_2(\xi), \mathbf{e}_3(\xi)$ in the vicinity of this extremum at $\xi = \xi_m$. The optimum rational normal–plane rotations on the intervals $[\,0, \xi_m\,]$ and $[\,\xi_m, 1\,]$ effectively cancel this "unnecessary" rotation, yielding an MTF with an angular velocity Ω_1 that is very close to the mean value $\overline{\Omega}_1$, as determined by the curve intrinsic geometry and the specified boundary conditions.

6 Closure

The problem of constructing an adapted orthonormal frame on a space curve (comprising the curve tangent and mutually orthogonal vectors in the normal plane), that exhibits minimal "twisting" between prescribed initial and final

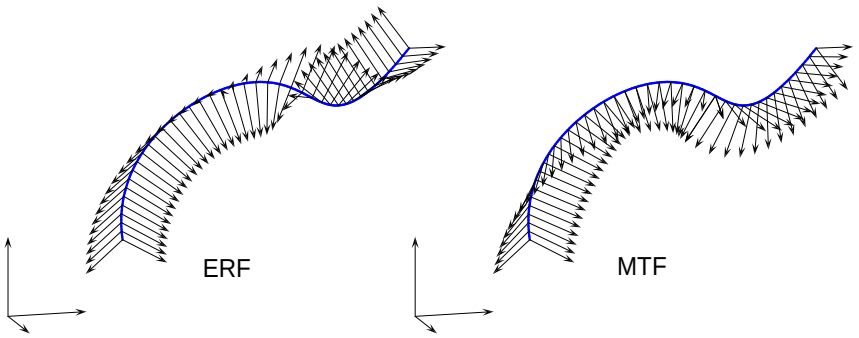

Figure 13: Comparison of normal–plane vectors of the Euler–Rodrigues frame (left) and the minimal twist frame (right) along the spatial PH quintic curve in Example 3. The initial ERF and MTF orientations are coincident.

instances, has been addressed. The Euler–Rodrigues frame (ERF) on spatial Pythagorean–hodograph (PH) curves offers a convenient point of departure for such constructions, since it is inherently rational and non–singular.

It was shown that, for spatial PH curves, the minimal twist frame (MTF) that satisfies the given boundary conditions and maintains a constant angular velocity component in the tangent direction admits a closed–form expression, although this incurs rather intricate transcendental terms. As an alternative, the strict imposition of a constant angular velocity component was relaxed, to permit the construction of *rational* MTFs on spatial PH quintics. By defining a rational MTF through a rational quartic rotation of the ERF normal–plane vectors, one can satisfy the boundary conditions and make the MTF angular velocity component agree with the constant mean value at both end points, with one residual scalar degree of freedom. Through a numerical optimization process, this free parameter can be used to minimize the root–mean–square deviation of the rational MTF angular velocity component about the mean value. This process yields rational MTFs of degree 8 on spatial PH quintics that are compatible with the boundary conditions and exhibit relatively mild variations of the tangent angular velocity component.

As a means of ensuring monotonicity of the rational MTF, or of further suppressing variations of the tangent angular velocity component, a strategy of subdividing the curve at the points that correspond to inflections and/or extrema of the ERF tangent angular velocity component was proposed. The "simple" variation of the ERF over the resulting subsegments allows a more

accurate compensation of the ERF variation by the rational normal–plane rotation that is employed to generate the MTF.

The algorithm described herein is relatively easy to implement, and yields simple (rational) solutions to the problem of smoothly varying the orientation of a rigid body along a given spatial path, compatible with prescribed initial and final orientations. A number of possible extensions of the algorithm come to mind. For example, one might consider the use of a cubic or higher–order complex polynomial $\mathbf{w}(\xi) = a(\xi) + \mathrm{i}\, b(\xi)$ — or complex spline function — to specify the rational normal–plane rotation (20) through expression (29). This offers additional free parameters to suppress the variation of $\Omega_1(\xi)$ about $\overline{\Omega}_1$. The basic methodology remains the same, but would require a computation–intensive solution of a non–linear multivariate optimization problem in order to determine appropriate values for these parameters.

References

[1] R. L. Bishop (1975), There is more than one way to frame a curve, *Amer. Math. Monthly* **82**, 246–251.

[2] L. A. Britton, W. K. Olson, and I. Tobias (2009), Two perspectives on the twist of DNA, *J. Chem. Phys.* **131** (24), Article 245101.

[3] R. P. Brent (1973), *Algorithms for Minimization Without Derivatives* Dover (reprint), Mineola, NY.

[4] G. S. Chirikjian (2013), Framed curves and knotted DNA, *Biochem. Soc. Trans.* **41**, 635–638.

[5] H. I. Choi and C. Y. Han (2002), Euler–Rodrigues frames on spatial Pythagorean–hodograph curves, *Comput. Aided Geom. Design* **19**, 603–620.

[6] M. R. Dennis and J. H. Hannay (2005), Geometry of Calugareanu's theorem, *Proc. Royal Soc. London* Series A, **461**, 3245–3254

[7] G. Farin (1997), *Curves and Surfaces for Computer Aided Geometric Design*, 4th edition, Academic Press, San Diego.

[8] R. T. Farouki (2008), *Pythagorean–Hodograph Curves: Algebra and Geometry Inseperable*, Springer, Berlin.

[9] R. T. Farouki (2010), Quaternion and Hopf map characterizations for the existence of rational rotation–minimizing frames on quintic space curves, *Adv. Comp. Math.* **33**, 331–348.

[10] R. T. Farouki (2016), Rational rotation–minimizing frames — Recent advances ond open problems, *Appl. Math. Comp.* **272**, 80–91.

[11] R. T. Farouki, G. Gentili, C. Giannelli, A. Sestini, and C. Stoppato (2017), A comprehensive characterization of the set of polynomial curves with rational rotation–minimizing frames, *Adv. Comp. Math.* **43**, 1–24.

[12] R. T. Farouki, C. Giannelli, C. Manni, and A. Sestini (2008), Identification of spatial PH quintic Hermite interpolants with near–optimal shape measures, *Comput. Aided Geom. Design* **25**, 274–297.

[13] R. T. Farouki, C. Giannelli, C. Manni, and A. Sestini (2012), Design of rational rotation–minimizing rigid body motions by Hermite interpolation, *Math. Comp.* **81**, 879–903.

[14] R. T. Farouki and C. Y. Han (2003), Rational approximation schemes for rotation–minimizing frames on Pythagorean–hodograph curves, *Comput. Aided Geom. Design* **20**, 435–454.

[15] R. T. Farouki, C. Y. Han, P. Dospra, and T. Sakkalis (2013), Rotation–minimizing Euler–Rodrigues rigid–body motion interpolants, *Comput. Aided Geom. Design* **30**, 653–671.

[16] R. T. Farouki and V. T. Rajan (1988), Algorithms for polynomials in Bernstein form, *Comput. Aided Geom. Design* **5**, 1–26.

[17] R. T. Farouki and T. Sakkalis (2010), Rational rotation–minimizing frames on polynomial space curves of arbitrary degree, *J. Symb. Comput.* **45**, 844–856.

[18] R. T. Farouki and T. Sakkalis (2012), A complete classification of quintic space curves with rational rotation–minimizing frames, *J. Symb. Comput.* **47**, 214–226.

[19] B. Jüttler (1998), Generating rational frames of space curves via Hermite interpolation with Pythagorean hodograph cubic splines, in *Geometric Modeling and Processing '98*, Bookplus Press, pp. 83–106.

[20] B. Jüttler (1998), Rotation minimizing spherical motions, in *Advances in Robot Kinematics: Analysis and Control* (J. Lenarcic and M. L. Husty, eds.), Springer, Dordrecht, pp. 413–422.

[21] B. Jüttler and C. Mäurer (1999), Cubic Pythagorean hodograph spline curves and applications to sweep surface modelling, *Comput. Aided Design* **31**, 73–83.

[22] J. S. Kim and G. S. Chirikjian (2006), Conformational analysis of stiff chiral polymers with end constraints, *Molec. Simul.* **32**, 1139–1154.

[23] F. Klok (1986), Two moving coordinate frames for sweeping along a 3D trajectory, *Comput. Aided Geom. Design* **3**, 217–229.

[24] M. Krajnc and V. Vitrih (2012), Motion design with Euler–Rodrigues frames of quintic Pythagorean–hodograph curves, *Math. Comput. Simul.* **82**, 1696–1711.

[25] E. Kreyszig (1959), *Differential Geometry*, University of Toronto Press.

[26] C. Mäurer and B. Jüttler (1999), Rational approximation of rotation minimizing frames using Pythagorean–hodograph cubics, *J. Geom. Graphics* **3**, 141–159.

[27] Z. Sir and B. Jüttler (2005), Spatial Pythagorean hodograph quintics and the approximation of pipe surfaces, in *Mathematics of Surfaces XI* (R. Martin, H. Bez, and M. Sabin, eds.) Springer, Berlin, pp. 364–380.

[28] J. Stoer and R. Bulirsch (2002), *Introduction to Numerical Analysis*, 3rd Edition, Springer, New York.

[29] J. V. Uspensky (1948), *Theory of Equations*, McGraw–Hill, New York.

[30] W. Wang and B. Joe (1997), Robust computation of the rotation minimizing frame for sweep surface modelling, *Comput. Aided Design* **29**, 379–391.

[31] W. Wang, B. Jüttler, D. Zheng, and Y. Liu (2008), Computation of rotation minimizing frames, *ACM Trans. Graphics* **27**, Article 2, 1–18.

[32] Z. Zheng and G. Wang (2005), Constructing rotation–minimizing frame of space Bézier curve, *J. Comput. Aided Design & Comput. Graphics* **17**, 1785–1792.